Penerbit Akademia Baru

Journal of Advanced Research in Fluid Mechanics and Thermal Sciences

Journal homepage: www.akademiabaru.com/arfmts.html
ISSN: 2289-7879

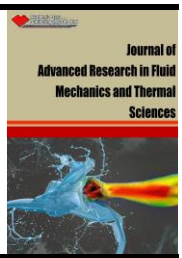

Parametric and Economic Analysis of a Pumped Storage System Powered by Renewable Energy Sources

Diego Penagos-Vásquez[1,*], Daniel Sanin-Villa[1]

[1] Faculty of Engineering, Department of Mechatronics and Electromechanics, Instituto Tecnológico Metropolitano, Robledo Campus, Calle 73 No. 76A-354, Vía al Volador, Medellín, Colombia

ARTICLE INFO

Article history:
Received 28 January 2021
Received in revised form 28 April 2021
Accepted 10 May 2021
Available online 26 June 2021

Keywords:
Store energy; electric generation; pumping systems; pelton turbines; hydraulic power

ABSTRACT

This article presents a mathematical model to calculate the cost and production of electrical energy of a system that combines energy storage through renewable sources such as wind and solar energy, applying a theoretical framework of mathematical aspects to evaluate a pumped storage system with Pelton turbines, using a novel methodology, easy to replicate. The results show that a greater increase in the diameter in the pipe of the pumping equipment reduces the electrical power supplied to the pump. On the other hand, the hydraulic losses in the pipe leading to the Pelton turbine are negligible for long lengths, so setting the maximum length instead of a variable-length with the hydraulic height does not affect the result. Finally, the information and explanation of each of the graphs that correlate to the variables of interest are shown. This seeks to offer a contribution to support technological development in areas that do not have electricity, taking advantage of natural resources.

1. Introduction

A way to store energy at times where there are moments of overproduction in the electrical generation systems is pumping water from a lower reservoir level to an upper level [1]. When it is necessary to produce electricity again, the pumps are turned off and stored water passes through a pipe and reaches a generating turbine, transforming the potential and kinetic energy into electricity that is delivered to the electrical grid. The energy consumed by pumps can come from surpluses in the power grid or renewable systems as photovoltaic or wind [2].

However, many people live without electricity, especially in rural or remote areas, which have searched for solutions to be able to provide electricity. This growing energy demand has led to important studies and projects to implement renewable energy sources, to minimize the negative environmental impact and the costs associated with conventional energy sources such as fossil fuels, which also contribute to the greenhouse effect, acid rain, and deforestation [3]. The International Energy Agency (IEA) gives a prediction of environmental consequences if there is no

* *Corresponding author.*
E-mail address: diegopenagos230276@correo.itm.edu.co

https://doi.org/10.37934/arfmts.84.1.4359

awareness of using new energy alternatives which would imply a 130% increase in CO2 emissions and 70% increase in oil consumption in 2050, which would bring an increase in the average global temperature of 6°C [4]. Also, the growth in electrification rates has increased from 76% in 1990 to 85% in 2012 worldwide [5].

Currently, it has been implementing the use of renewable energies through technological development [6], supporting the seventh of Sustainable Development goals set by the United Nations Development Programme (UNDP) for 2030 [7]. According to the study by Khosravi *et al.,* [8], at the end of 2017, the renewable generation capacity was 2179 GW and continues with an annual growth of 8 to 9%. There are various types of renewable energy, where the most common are photovoltaic and wind, which seek to take advantage of naturally occurring resources such as the sun and air and through these generate a transformation that allows exploitation and uses for various purposes [9]. Solar energy is an abundant resource that can be harnessed with a direct incidence [10]. On the other hand, the conversion can be done using a hybrid photovoltaic thermal air, where electricity and heat can be obtained at the same time [11]. In analogy, wind can be related as a derivative of solar energy, because it is the effect of the heating of the atmosphere and the rotation of the planet. The speed with which the air moves can be harnessed to generate electricity through the movement of a wind turbine [12].

Nevertheless, the problem arises when the production of energy from renewable sources is not used immediately or when the generation occurs unpredictably due to the change in climatic conditions, generating intermittent energy delivery. These aspects of renewable energies reduce reliability due to a lack of control [13].

This is the reason why a storage system is considered, which is responsible for supplying the need for energy during peak demand times, where the water stored is released to a lower reservoir and transformed into electrical energy through a turbine. At times of low energy demand, the pump works to store energy in the form of water accumulated in a reservoir at a higher level, avoiding the intermittency generated by renewable sources [14]. Therefore, when there is uncertainty of availability from renewable sources, the energy stored in the reservoir is used to stabilize the output power, serving as a backup system when renewable energies are not available.

When making combinations of hydroelectric systems with renewable sources, a promising solution for the energy balance in the future of electric energy based on renewable energy is given [15]. Also, hydraulic energy has proven to be reliable due to its stability in the market and its high growth in world demand [16]. Figure 1 shows a simplified scheme of the operation of these coupled generation and storage systems, showing the direction of the flow.

The combination of renewable energy types with hydraulic energy storage system has been studied, giving encouraging results. It has been investigated the integration of photovoltaic system (PV) and pumped-storage hydroelectricity (PSH), through a techno-economic analysis, giving as result a saving up to 18.2% for the storage by batteries [18]. An integrated economic study has also been carried out on Photovoltaic arrays and wind turbine, for the supply of electric energy to a coastal community, where the results showed the final cost of 0.27 $/kWh, much lower than the 0.95 $/kWh operating a diesel generator [19].

The objective of this work is to perform a parametric analysis of a pumped storage system powered by renewable energy sources, by means of graphs programmed in engineering software, to describe the behavior of the system through geometric, physical, and economic variables, in order to support remote areas that do not have access to electricity through the conventional power grid. It should be noted that the emphasis will be on the centrifugal pump and the Pelton turbine, and not on the renewable energy sources that feed the system. Likewise, this work provides a complete and clear framework of the mathematical aspects to evaluate a storage system pumped with Pelton turbines, applying a novel methodology, easy to replicate.

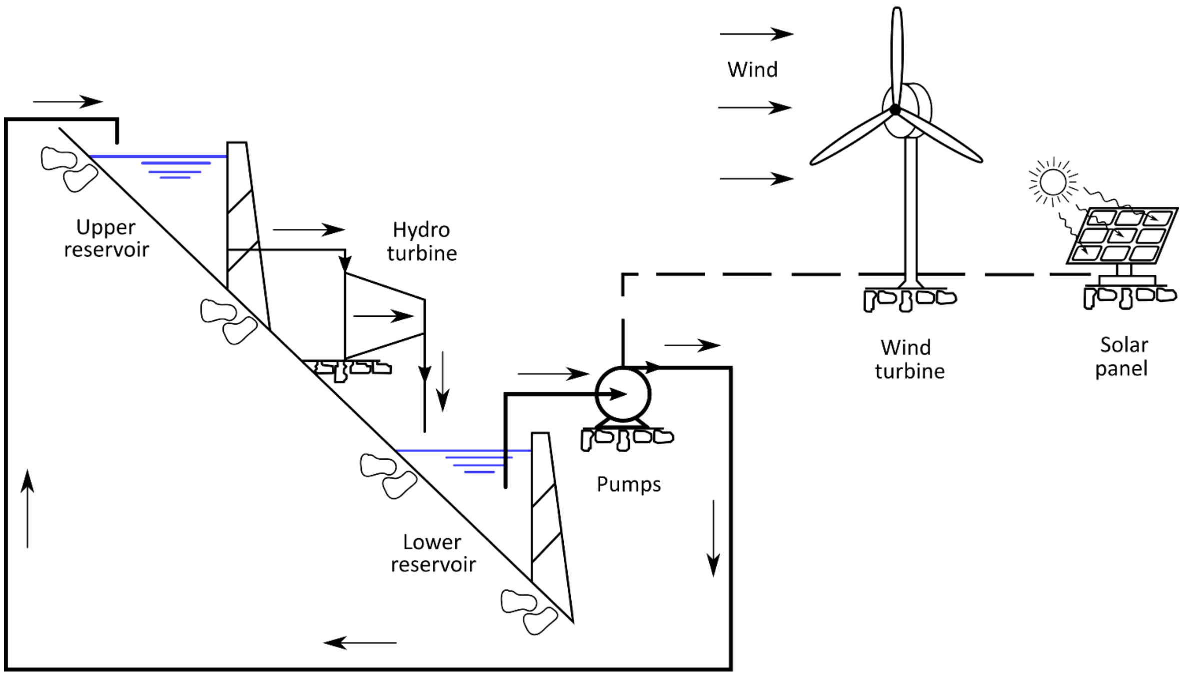

Fig. 1. Scheme of storage generation from wind and solar energy [17]

2. Methodology

In the development of the model, it will be assumed that renewable energy sources feed the pumping system and they will work intermittently for a whole month. The system proposed in this work is composed of two stages: first, the elevation of a quantity of water from the lower storage place to the upper reservoir, and subsequently, hydroelectric generation from the fall of water from the upper reservoir, through a generation Pelton turbine. A mathematical model will be presented through macroscopic energy and mass balance equation, and electric transformation systems. Transmission and distribution losses will not be considered.

Finally, the term reservoir height emphasizes the difference in head between the pump discharge and the highest point of pumping, while hydraulic height is the difference between the surface of the water stored in the reservoir and the nozzle.

2.1 Model for the Pumping System

Fluid conduction systems within pipelines have been extensively studied, and the constitutive equations can be deduced simply by complying with the conservation equations of mass, momentum, and energy. In this analysis, the flow rate is used instead of mass flow since temperature and density changes are negligible because water is considered an incompressible fluid. The equation for Hydraulic Power required to raise the fluid in a height starts from the equation of scalar (one-dimensional) energy in the direction of flow, and the Darcy equation for the solution of the speed equation and friction losses.

Eq. (1) is applied to obtain the dimensionless friction factor f, where the Swamee-Jain equation is used, valid in turbulent flow regime (5E+3 ≤Re≤ 1E+8), which has an accuracy of ±1.0%

concerning Colebrook-White expression. In this case, ∈ [m] is the roughness of the pipe material, D [m] is the internal diameter of the conduction pipeline, and Re is the dimensionless number [20].

$$f = \frac{0.25}{\left[\log\left(\frac{\epsilon}{3,7 \cdot D} + \frac{5,74}{Re^{0,9}}\right)\right]^2} \tag{1}$$

Reynolds dimensionless number Re relates the inertial viscous forces. In general, Re<2000 indicates a laminar flow, while a higher number is turbulence flow. Reynolds number is defined in Eq. (2), where ρ [kg/m³] is the density of the fluid, μ [kg/m·s] the dynamic viscosity, and V [m/s] the magnitude of the average velocity within the pipe [21].

$$Re = \frac{\rho D V}{\mu} \tag{2}$$

Now performing the steady-state energy balance for the conduction of water from the lower intake to the upper reservoir is obtained through Eq. (3). Points a and b are located on the fluid free surface in the lower and upper reservoir, respectively.

Pressure P [Pa], which can be considered manometric and equal to 0 Pa for points considered, γ is related with specific weight [N/m³]. Height Z [m] corresponds to the term of gravitational potential energy, pipe length L [m] is the distance between points evaluated, and the gravity g [m/s²]. Finally, the Pump head H_p [m] is the energy added to the fluid by a pump. The Darcy-Weisbach equation relates hydraulic losses, so it is considered for this analysis [22].

$$\frac{P_a}{\gamma} + Z_a + \frac{V_a^2}{2g} - f\frac{L}{D}\frac{V^2}{2g} + H_p = \frac{P_b}{\gamma} + Z_b + \frac{V_b^2}{2g} \tag{3}$$

To calculate the value of hydraulic pumping power P_{pump} [W], Eq. (4) is used, where Q [m³/s] relates to the flow [23].

$$P_{pump} = \gamma Q H_p \tag{4}$$

The electrical power required to supply the pump P_e [W] is defined in Eq. (5), where η_{pump} is the pump efficiency, delivered by the manufacturer.

$$P_e = \frac{P_{pump}}{\eta_{pump}} \tag{5}$$

2.2 Model for the Pelton Turbine Generation System

Pelton turbines take advantage of the energy of the fluid coming from a considerable height so that the flow rate is not very large. The Bieudron hydroelectric power plant, located in the Swiss Alps, is the largest in the world with a hydraulic height of 1883 m [24]. This is the reason why it is preferred instead of the Francis turbine and even the pump operating as a turbine (both require a higher flow rate), even though it is more expensive to install [25]. On the other hand, it is advisable to use a radial-flow centrifugal pump instead of a mixed-flow or axial-flow, because the radial-flow pump is designed to lift the fluid to considerable heights, but with a lower flow [26].

The equations to determine the power of hydraulic generation correspond to the well-known Euler equations, which are simplified expressions of the momentum and energy equations coupled for incompressible fluids. If the viscous effects are not considered, it can be assumed that the relative velocity of the fluid after meeting the bucket does not change its magnitude, only its direction. This generates a momentum change on the Pelton wheel. In Figure 2, (a) shows the interaction scheme between the fluid and the turbine cannons, (b) presents the blade cross-section in one bucket.

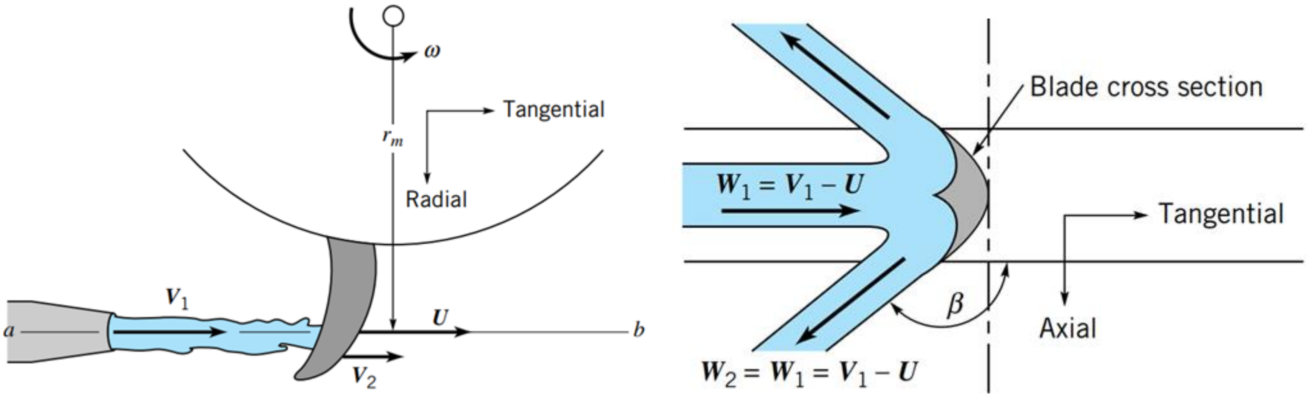

(a) (b)

Fig. 2. Fluid-cannon interaction in (a) Pelton turbine and (b) Bucket cross-section [27]

Eq. (6) and Eq. (7) are the mathematical expressions to calculate torque $T_{Turbine}$ [Nm] and power $P_{Turbine}$ [W] in terms of geometric parameters of the Pelton turbine, where β [°] is the angle between the water flow, r_m is the Pelton turbine radius, V_1 [m/s] is the nozzle exit velocity (determined with Eq. (3)), and U [m/s] is the tangential speed of the bucket.

$$T_{Turbine} = \rho Q(U - V_1)(1 - \cos\beta)r_m \quad (6)$$

$$P_{Turbine} = \rho QU(U - V_1)(1 - \cos\beta) \quad (7)$$

To obtain the maximum power extracted P_{Max} [W], the above equation for velocity is derived and equals zero. When performing this process, it is found that the maximum velocity value U_{max} [m/s] is presented in Eq. (8). In this way, the maximum power would be expressed in Eq. (9). Besides, it is possible to express the flow rate as a function of the velocity.

$$U_{max} = \frac{V_1}{2} \quad (8)$$

$$P_{Max} = -\rho Q\left(\frac{V_1}{2}\right)^2(1 - \cos\beta) \quad (9)$$

2.3 Water Accumulation

To determine the amount of water that is available in the upper reservoir, a mass balance is performed in a transitory state according to Eq. (9). As mentioned above, water is an incompressible fluid. Therefore, Eq. (10) can be expressed in terms of the volumetric flows of input and output as presented in Eq. (11).

$$\dot{m}_{in} - \dot{m}_{out} = \frac{dm_{VC}}{dt} \quad (10)$$

$$Q_{in} - Q_{out} = \frac{dVC}{dt} \tag{11}$$

It is possible to consider the volume VC [m³] as a function of the water level N [m] in the reservoir by Eq. (12), where $A(N)$ [m²] is the variation of the cross-sectional area of the reservoir depending on the water level.

$$VC(N) = N * A(N) \tag{12}$$

2.4 Operating Revenue and Sale

The revenue of electric energy $Cost_p$ [$] used by the pumps will be calculated in Eq. (13), where t_p [hrs] is a monthly working time of the pumping system, and C_p [$/kWh] is the unitary value. Similarly, to determine the sales value of the energy generated by the turbine system $Cost_t$ [$], Eq. (14) is applied, where t_t [hrs] is a monthly working time of the turbine, and C_t [$/kWh] is the unitary value.

$$Cost_p = P_e * t_p * C_p \tag{13}$$

$$Cost_t = P_{Max} * t_t * C_t \tag{14}$$

2.5 Initial Conditions

Table 1 shows the parameters configured to obtain the calculating the performance and cost of electric energy and power production in a system of the pump and the Pelton turbine. Sub-index p denotes the variables related to the pump, while sub-index t for the turbine.

Table 1
Parameters configurated for the analysis

System	Variable	Value
Pump	D_p [m]	0.6-1.0
	L_p [m]	100 + Reservoir height
	η_{pump} [%]	85
	t_p [hrs]	200
	C_p [COP/kWh]	140-220
Pelton Turbine	f_t [-]	0.02
	L_t [m]	1020
	D_{1t} [m]	0.9
	D_{2t} [m]	0.2
	β [°]	165
	t_t [hrs]	400
	C_T [COP/kWh]	340-500

The properties used for water are density $\rho = 997$ kg/m³, dynamic viscosity $\mu = 8.91$E-4 kg/m·s at 25°C [28], specific weight $\gamma = 9780$ N/m³. The roughness ∈ is 1.5E-4 m, for galvanized steel pipe [23]. Pump efficiency η_{pump} of 85% is assumed. The length of the pumping system pipe L_p is assumed to be 100 m initial, according to the horizontal pipeline in Figure 1.

On the other hand, the cost of electricity generation and sale is taken from the energy service company EPM, of Colombia. Table 2 shows the variation in the price of electricity between 2012 and 2020, using the local currency (COP) [29]. Therefore, the unit value is considered in the range 140-220 COP/kWh for generation and 340-500 COP/kWh for sale, to compare the consumption of the pump with the energy generated by the turbine. For this analysis, transmission and distribution losses will not be considered.

3. Results
3.1 Pump System

Considering the mathematical model, a code is developed in Engineering Equation Solver (EES) that allows to simultaneously solve the equations defined in the prior section. The results are presented using graphs, where the trend is observed as the parameters of flow, reservoir heigh, speed of exit of the nozzle, the cost of production of energy, and the cost of sale are modified.

Figure 3 shows the power required by the pump system [MW] for different flow rates [m^3/s], maintaining a height difference value from the lower to the upper reservoir equal to 400 m, using Eq. (1)-(5). The blue bar graph refers to hydraulic power, while the red dot graph is electrical power. Both have a growing trend but no linear tendency, where the electrical and hydraulic power required by the pump increases much more often than the flow rate. In an analysis, the power difference, although it seems to be increasing, is conditioned by the efficiency of the pump. Also, the pump requires more power to raise a greater flow. If a flow of 3 m^3/s is pumped, at least 18.5 MW of power is required, while the flow rate is 1.5 m^3/s, the power would be 8 MW, which means that this must be the power delivered to the centrifugal pump or a group of these. The flow pumped to the upper reservoir can have considerable variations depending on the amount of water and energy that is required to be stored in the upper part.

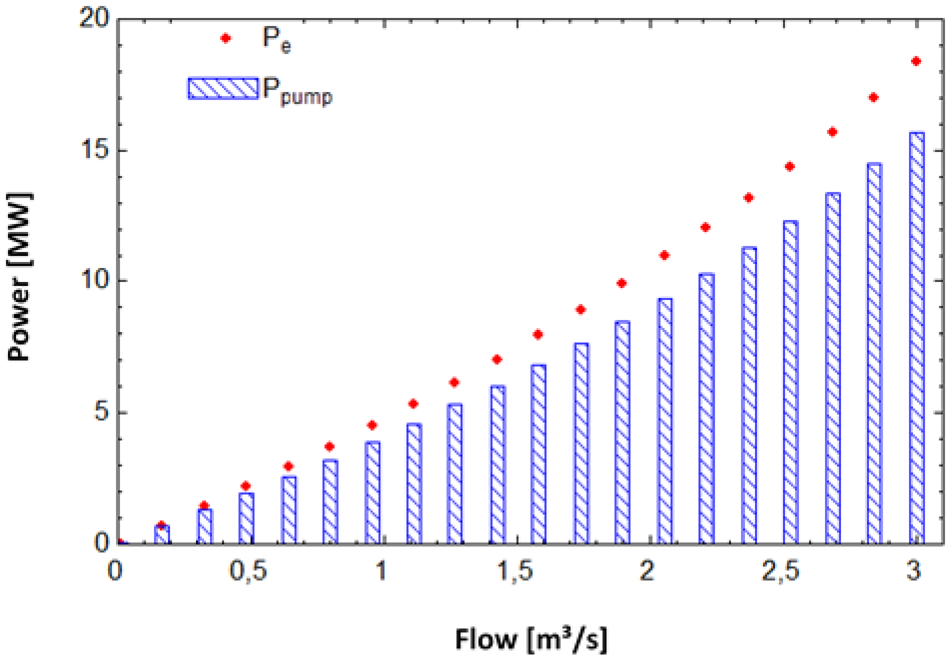

Fig. 3. Electrical and hydraulic power of the pumping system

The following is a comparison between the consumed electric power [MW] with the variation of the reservoir height [m]. Eq. (1)-(5) were used. Figure 4 kept the pipe diameter constant at 0.6 m, while Figure 5 was 1.0 m. Both graphs show different colored scatter curves for each of the analyzed flow rates, from 1 m^3/s to 4 m^3/s in intervals of 1 m^3/s, where a linearly increasing behavior is observed. It is possible to see that the higher the flow rate, the more power the pump consumes, regardless of the pipe diameter selected. On the other hand, it can be noted that when using a larger diameter (Figure 5), the electrical power supplied is lower. This is because the hydraulic losses decrease, showing that if a higher flow rate is required, it is advisable to use larger diameters to reduce the electrical power input. The pipeline length is set at 100 m plus the reservoir height, where this initial power is to overcome the hydraulic losses of the initial distance before pumping to a specific reservoir height. Finally, a gradual difference increase considerably in the power input is observed as the flow demand and reservoir height increase. Looking at Figure 4, for the 400 m reservoir height, the difference between the 4 and 3 m³/s curves is 10.85 MW, while in Figure 5 it is 5.06 MW.

It should be clarified that the diameters analyzed are not practical, so they are assumed to be the sum of the diameters used for the number of pumps being operated. Considering the high powers required, this situation should not be replaced by a single pump, so it is suggested to use parallel systems that reduce the flow rate that each pump must drive and therefore proportionally reduce the power of each. The algebraic sum of the pump powers must be equal to the total hydraulic power demanded by the system to transport a certain amount of flow and elevation. Finally, it is emphasized that the pumping head must be greater than the hydraulic height of the Pelton turbine.

Figure 6 shows the growth of hydraulic losses (using the Darcy-Weisbach equation) [m] for different values of reservoir height [m]. The variation in pipe length was kept the same as in Figure 4 and Figure 5. Eq. (1)-(3) was used to construct the graph. Four curves of different colors are observed, where each one represents a different flow rate.

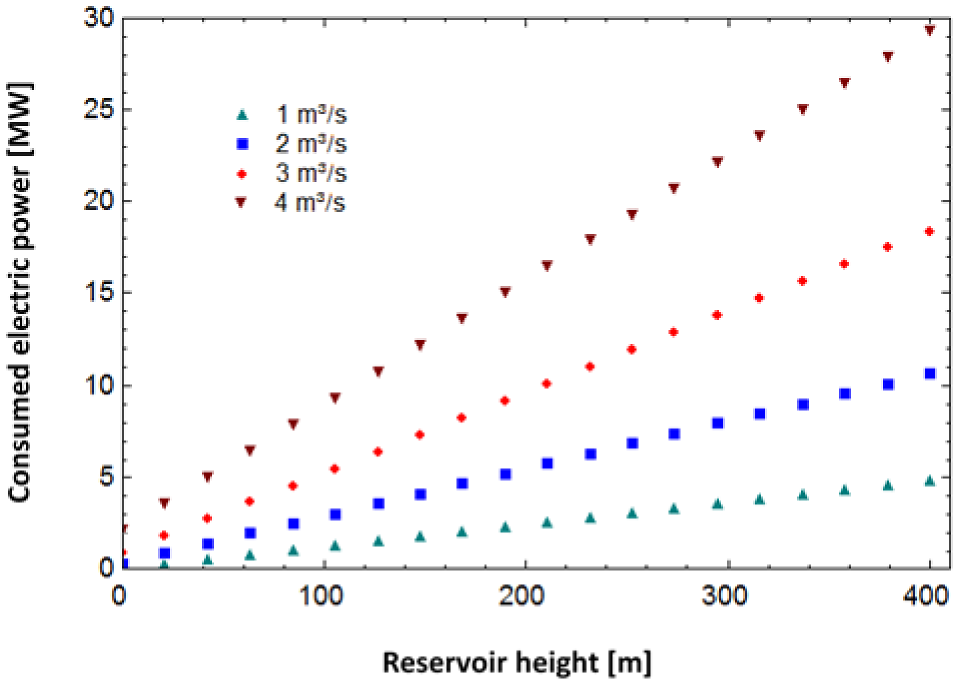

Fig. 4. Electrical power consumed with the variation of the flow, using D_p=0.6 m

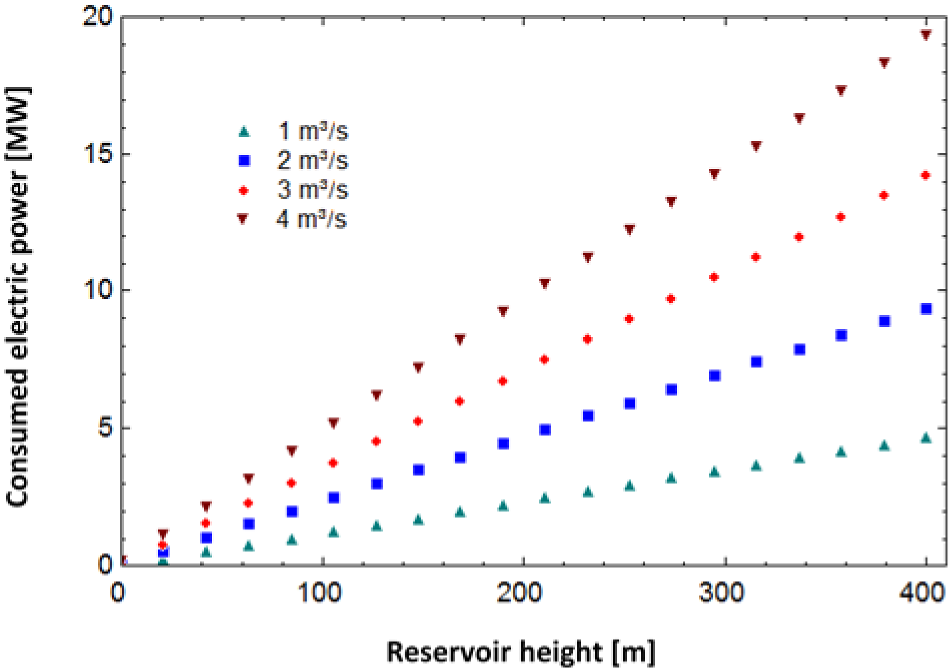

Fig. 5. Electrical power consumed with the variation of the flow, using D_p=1.0 m

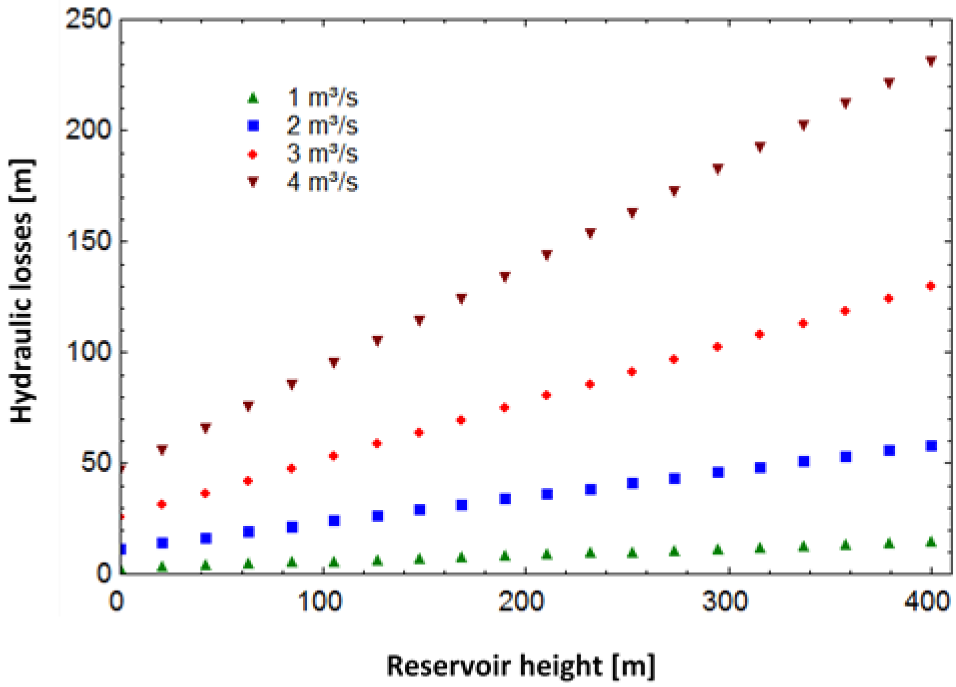

Fig. 6. Variation of hydraulic losses by reservoir height

In detail, the hydraulic losses tend to increase as the reservoir height increases, because the length of the pipe is proportional to the losses. On the other hand, using a constant pipe diameter, the increase in flow rate causes the losses to increase considerably. This is since the velocity increases with the square of the flow rate because they are related, increasing the turbulence. Consequently, when analyzing the 3 and 4 m^3/s curves for a reservoir height of 400 m, an additional 101.1 m of pumping is required, while for the same height between the 1 and 2 m^3/s curves, the difference is 42.73 m. Finally, it is mentioned that the hydraulic losses when the reservoir height is 0 m are those required to overcome the friction of the initial 100 m of the pipeline. It is observed that the effect of the flow rate is considerable when at 21 m of the pumped head (121 m of pipe length) the losses are 55.96 m at 4 m^3/s, which is like having a pumped head of 400 m (500 m of pipe length), where 57.18 m at 2 m^3/s are required.

3.2 Pelton Turbine

Figure 7 shows the change in nozzle velocity (V1 in Figure 2) [m/s] and hydraulic losses [m] with the turbine hydraulic height [m], using Eq. (3). Three curves can be observed, representing the velocity, the losses with a constant (1020 m), and variable pipe length, depending on the hydraulic height, where the trend is increasing in the analyzed range. Hydraulic height corresponds to the vertical distance from the highest point of the upper reservoir to the water outlet at the nozzle of the Pelton wheel. The non-linear effect of the velocity increase at this point is mainly due to the existence of viscous dissipation phenomena inside the fluid and to friction losses due to rubbing with the pipe. These losses are encompassed by the friction factor f_t. It can be detailed that the nozzle velocity increases slowly at high heads, while the losses tend to increase. As can be seen, when using the variable height, there is a difference between the hydraulic losses, which is minimized as the hydraulic height increases. For example, for a height of 538.4 m (velocity of 100 m/s), there is a loss difference of 13.69 m between the curves. This may seem like a lot, but it represents an error of 2.6%, with the real head being 524.7 m. The constant pipe length was used for the velocity curve. However, using this methodology for higher heights is feasible if it is desired to maintain the pipe length and evaluate other variables of interest. On the other hand, when comparing the present graph with Figure 6, the hydraulic losses are much lower, because gravity and flow direction go in the same direction and this helps the fluid, minimizing the losses.

Figure 8 presents the hydraulic power generated [MW] for the variation of hydraulic height [m], for different nozzle diameters. Eq. (3) and (9) were used to generate the graph, where the nozzle velocity was varied between 0-100 m/s. A group of curves pertaining to the nozzle diameter analyzed is observed. The trend for each curve is exponential, where it is observed that as more hydraulic height the power generated increases. Each curve was made for nozzle diameters of 0.1 m, 0.2 m, 0.4 m, 0.6 m, and 0.8 m, showing that the 0.4 m nozzle allows obtaining a hydraulic power up to 24.63 MW at 500 m hydraulic height, being the highest of all, where it is followed by the 0.2 m nozzle with 15.39 MW, nozzle that remained constant for the other analyzed graphs. On the other hand, it is not justifiable to have 0.8 m and 0.1 m diameter nozzles, since they allow obtaining a maximum of 4 MW, wasting up to 11.4 MW with respect to the 0.2 m nozzle. Finally, when comparing with Figure 5, it is observed that the power generated is lower than the power consumed by the pump because the hydraulic losses are higher for the turbomachine. Likewise, for the following analysis, the nozzle diameter of 0.2 m will be maintained. Finally, it is mentioned again that the hydraulic height must be less than the head pumped by the turbomachine.

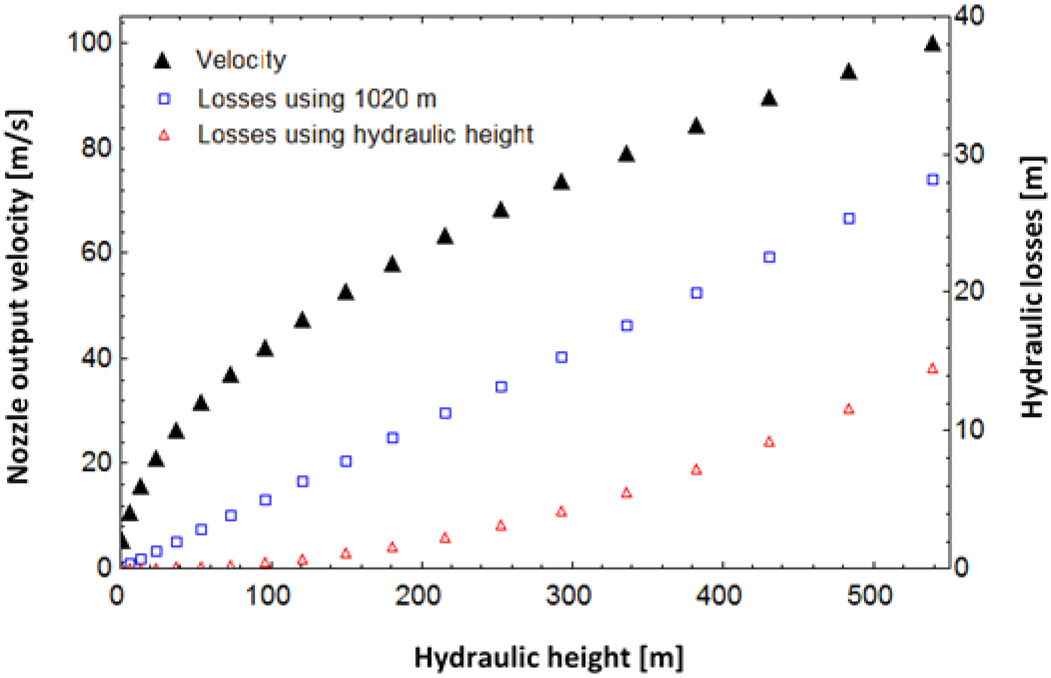

Fig. 7. Nozzle output velocity and hydraulic losses as a function of hydraulic height

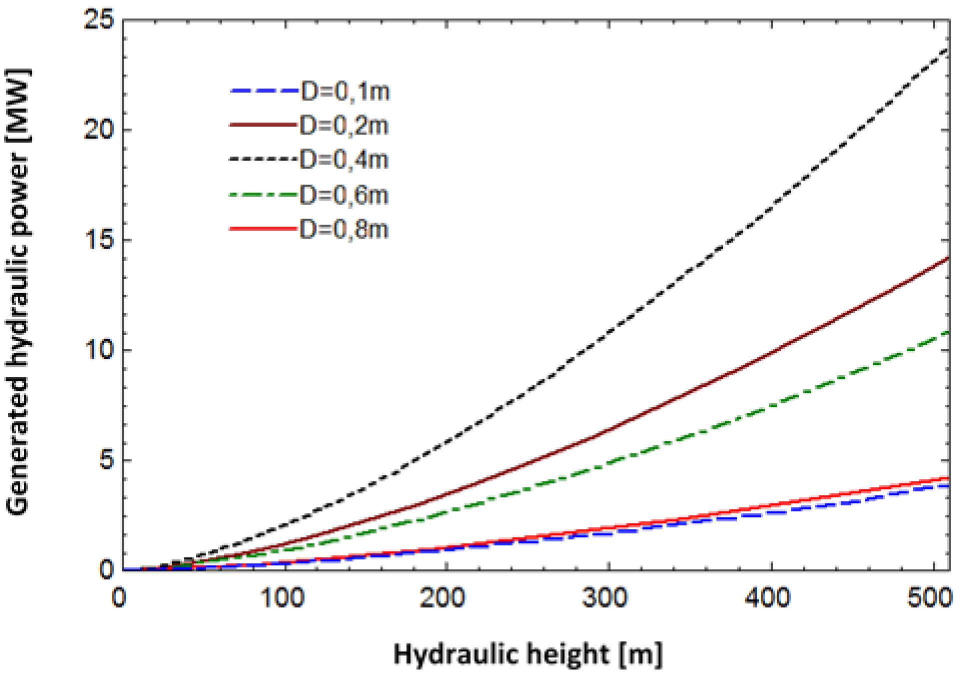

Fig. 8. Generated hydraulic power as a function of hydraulic height

3.3 Economic Analysis

Below is the financial analysis of the electric power consumption of the centrifugal pump. Figure 9 shows the variation of the operating cost [COP-million] with the variation in the flow rate [m³/s], for different purchase prices for generation only, not including transmission losses, shown in more detail in Table 2. Eq. (1)-(5) and Eq. (13) were used for the calculation, keeping the reservoir height constant at 400 m and the parameters of Table 1, highlighting the monthly operating time of 200 hours, more than 6 hours per day. Five curves associated with a price for consumed electricity (kWh) are shown for Colombian currency (COP). A non-linear increasing behavior is observed, which shows the increase in the operating cost of the pump by requiring a greater flow demand. It is predictable to determine that the higher the cost of energy, the higher the operating cost, so the increase is proportional if the price doubles, since the electrical power analyzed is the same for all five cases, starting from the graph shown in Figure 3. On the other hand, an exponential increase can be noticed. Finally, at 220 $/kWh, a maximum operating cost of COP 812.4 million is estimated if the electricity grid were used, so this amount must be recovered with the Pelton turbine to offset the cost and generate profits.

Table 2
Variation in the price of electricity between 2012 and 2020

Year	Cost of generation [COP/kWh]	Cost of sale [COP/kWh]
2012	134.28	337.34
2013	138.14	334.81
2014	143.77	354.20
2015	161.84	394.60
2016	165.38	437.01
2017	168.00	435.32
2018	168.49	461.90
2019	201.84	481.17
2020	216.46	534.43

Similarly, Figure 10 shows the variation of the operating cost [COP-millions] for the variation of the reservoir height [m]. The flow rate was kept constant at 3 m³/s. An increasing linear behavior is observed, so the increase in cost is proportional to the height at which the fluid is pumped. As in Figure 6, when the reservoir height is zero, the operating cost is between 126 and 200 million COP, because it is the cost of the initial 100 m length of the pipe. Finally, the cost when the height is 400 m is equivalent to the cost of 3 m³/s shown in the graph of Figure 9.

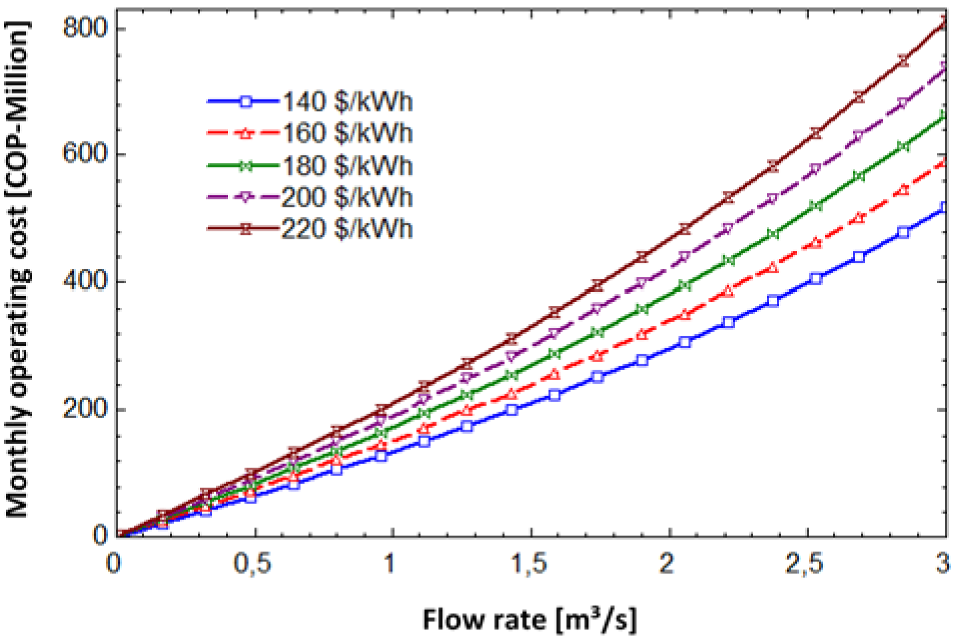

Fig. 9. Cost of operation as a function of the flow rate variation, for different unit values of energy cost

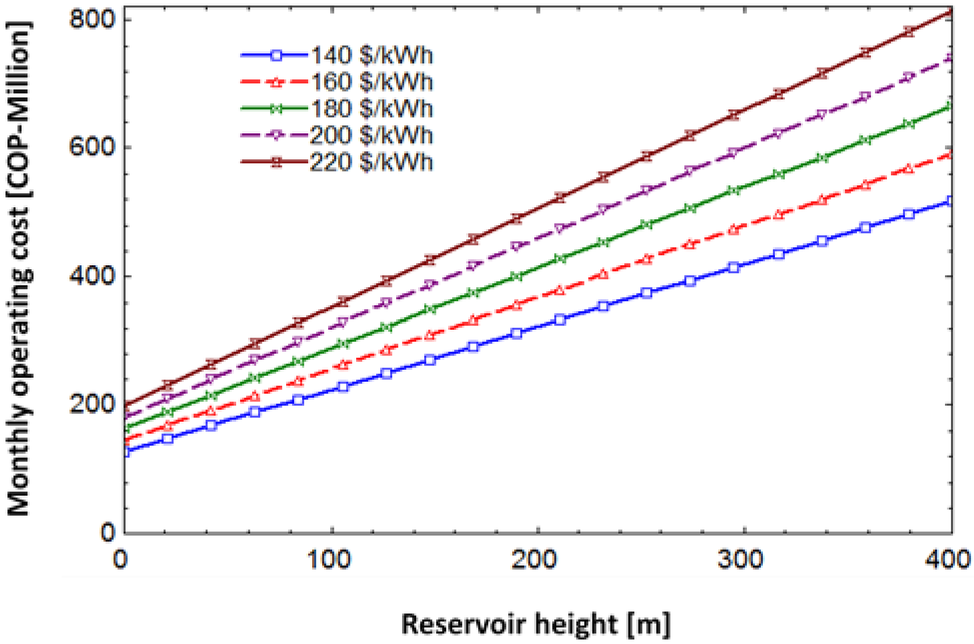

Fig. 10. Cost of operation as a function of the reservoir height, for different unit values of energy cost

The next figures show the financial analysis of the Pelton turbine profit, employing Eq. (3), (9), and (14). Figure 11 shows the variation of the operating cost [COP-millions] with the flow [m³/s] of the Pelton turbine, for different sales prices, according to the balance of the sales of the last 8 years In Colombia. In this case, 400 hours of work per month are assumed, equivalent to 13 hours per day. A group of five curves associated with the sale price of electricity for the Colombian currency can be displayed. It is observed that each one of the electricity generation profit curves increases exponentially with the increase in the flow rate (which is proportional to the increase in hydraulic height), being more noticeable between flows of 2 and 3 m³/s. This is because the hydraulic losses are negligible. After all, water goes in the same direction as gravity. Also, the trend is proportional to the hydraulic power generated, which can be seen in Figure 8. The maximum profit (if it is sold at 500 $/kWh), if 3 m³/s circulates at the output is COP 2681 million, this for a hydraulic height of 491 m.

On the other hand, when comparing the cost of sale and the cost of operation of the pump, encouraging results can be obtained. In Figure 9, the maximum operating cost of the pump is COP 812.4 million (at 220 $/kWh, 3 m³/s, reservoir height 400 m), while the minimum profits generated from the Pelton turbine is COP 1306 million (at 340 $/kWh, 2.68 m³/s, hydraulic height of 393 m), giving a difference of COP 493.6 million of profits at least for similar heights.

Finally, Figure 12 shows a similar scheme, but the variation is made about the hydraulic height. For this graph, the outflow was kept constant at 3 m³/s, showing the curves with the same sales values as in Figure 11. An increasing linear behavior is observed, which increases in proportion to the price. Unlike in Figure 10, when the hydraulic height is zero there are no gains because the energy of the water (kinetic and potential) does not produce work in the Pelton turbine. As the height increases, the energy contained in the water passes directly to the turbine to transform it into electrical power, so the energy generated is used for sale or consumption itself. For the data in the analysis, it is possible to obtain profits between 1931 and 2840 million COP, but this at a hydraulic height of 520 m. If the turbine is kept close to 400 m of pumping difference (Figure 10), at a consumption price of 220 $/kWh, the electricity cost is 738 million COP, while the turbine at a hydraulic height of 395 m, at a sale price of 340 $/kWh it is obtained from COP 1.465 million, obtaining profits of COP 727 million.

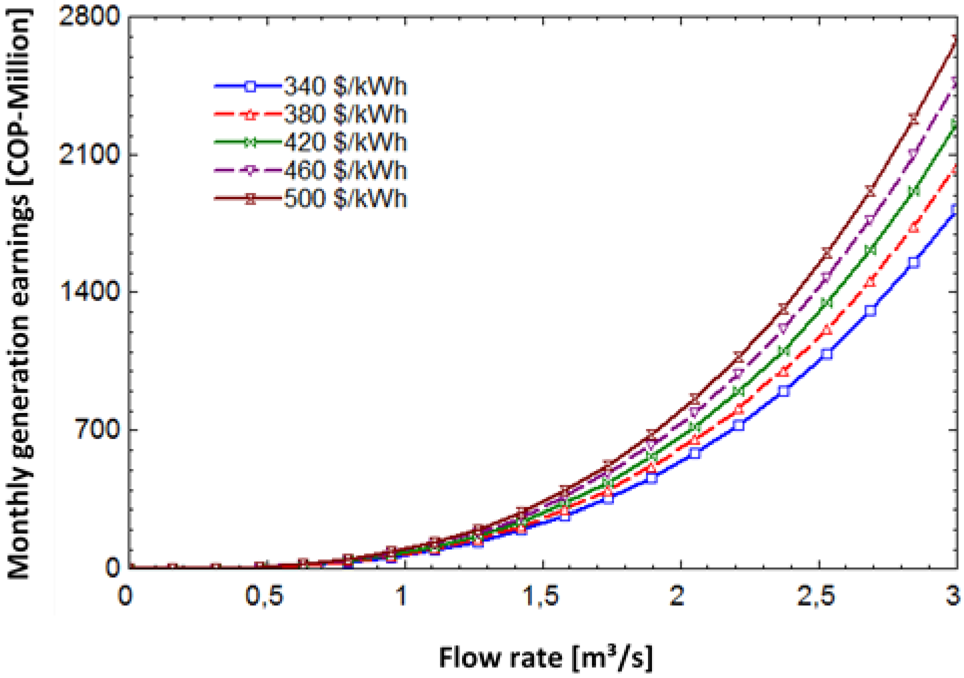

Fig. 11. Energy sales value in function of the flow rate, for different unit energy values

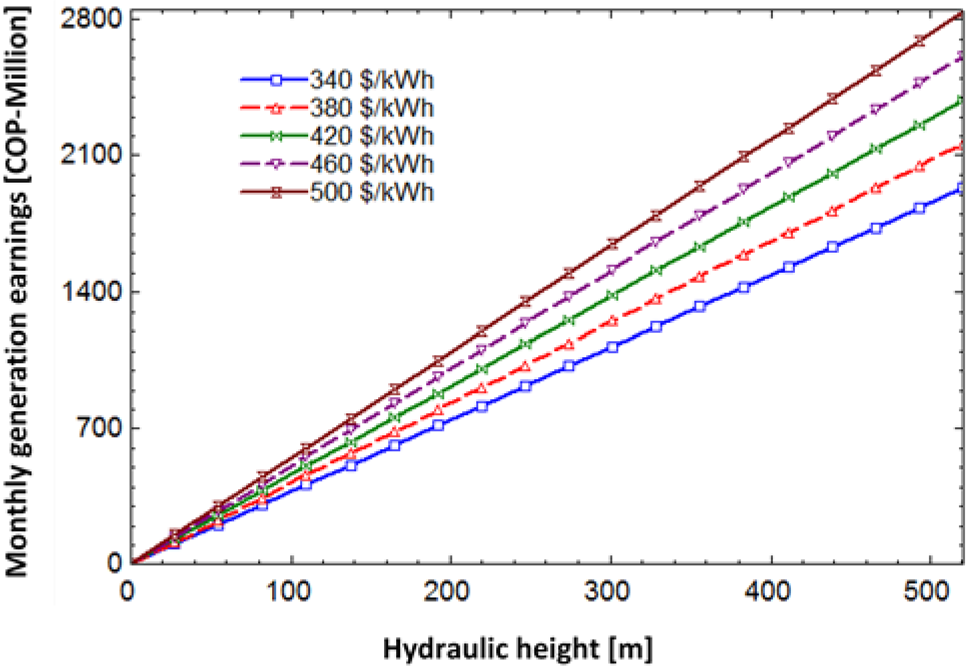

Fig. 12. Energy sales value in function of the hydraulic height, for different unit energy values

4. Conclusions

A mathematical model is proposed for energy storage through a water reservoir using renewable energy; Likewise, the analysis of the variation of consumptions and power generation according to the height of the pumping and generation system, respectively.

For the pumping equipment, it is evident that increasing the diameter of the pipe that leads the water to the reservoir, allows reducing the electrical power of the pump for the same flow. A reservoir height of 400 m and a flow rate of 4 m³/s, for a diameter of 0.6 m, the power consumed is 29.31 MW, while a diameter of 1.0 m is 19.3 MW, obtaining a saving of 10 MW.

For the Pelton turbine, hydraulic losses are shown to be relatively insignificant, so the analysis can be simplified by establishing a constant pipe length with minimal error, even if the hydraulic height is less. If you have a flow velocity of 100 m/s, with a fixed pipe length of 1020 m, it is obtained that a hydraulic height of 538.4 m generates hydraulic losses of 28.2 m, while a variable pipe length gives as a result, a hydraulic height of 524.7 m and losses of 14.51 m, obtaining an error of only 2.6%. Finally, the diameter of the nozzle is relevant to the power generated. When carrying out a parametric study, it is shown that having a hydraulic height of 500 m, the 0.4 m diameter nozzle produces about 24 MW, well above the 0.1 m and 0.8 m nozzles that reached a maximum of 4 MW.

In the economic analysis, the electrical consumption of the pump, and the benefit of the Pelton turbine are investigated. Specifically, the operation of the pump at 220 $/kWh, 3 m³/s, reservoir height 400 m, represents a cost of 812.4 million COP, while a similar point of operation of the turbine at 340 $/kWh, 2.68 m³/s, hydraulic height of 393 m yields profits of 1306 million COP, giving a difference of COP 493.6 million of profits at least for similar heights.

On the other hand, electricity generation can be carried out using turbines other than the Pelton type, which use lower hydraulic height but consume greater flow. In this way it is possible to have systems with shorter conduit pipes, but with a larger diameter.

Finally, the use of hybrid systems of renewable energy sources with hydraulic storage systems has been shown in the literature. The impact is that remote populations that do not have direct access to conventional grid supply can take advantage of the energy sources available in the area. The pumped storage system becomes relevant as a means to store energy. When there is a high demand from renewable sources, the surplus energy is used to operate the centrifugal pump, while when there is low demand, the Pelton turbine is put into operation, using the reserved water as feed, stabilizing the output energy that will be used by the population.

Acknowledgment
The authors wish to thank the reviewers for their valuable input and suggestions from this research.

References

[1] Sun, Kaiqi, Ke-Jun Li, Jiuping Pan, Yong Liu, and Yilu Liu. "An optimal combined operation scheme for pumped storage and hybrid wind-photovoltaic complementary power generation system." *Applied energy* 242 (2019): 1155-1163. https://doi.org/10.1016/j.apenergy.2019.03.171

[2] Luo, Xing, Jihong Wang, Mark Dooner, and Jonathan Clarke. "Overview of current development in electrical energy storage technologies and the application potential in power system operation." *Applied energy* 137 (2015): 511-536. https://doi.org/10.1016/j.apenergy.2014.09.081

[3] Jurasz, Jakub, Paweł B. Dąbek, Bartosz Kaźmierczak, Alexander Kies, and Marcin Wdowikowski. "Large scale complementary solar and wind energy sources coupled with pumped-storage hydroelectricity for Lower Silesia (Poland)." *Energy* 161 (2018): 183-192. https://doi.org/10.1016/j.energy.2018.07.085

[4] Khalkhali, Masoumeh, Kirk Westphal, and Weiwei Mo. "The water-energy nexus at water supply and its implications on the integrated water and energy management." *Science of the Total Environment* 636 (2018): 1257-1267. https://doi.org/10.1016/j.scitotenv.2018.04.408
[5] Pali, Bahadur Singh, and Shelly Vadhera. "A novel pumped hydro-energy storage scheme with wind energy for power generation at constant voltage in rural areas." *Renewable energy* 127 (2018): 802-810. https://doi.org/10.1016/j.renene.2018.05.028
[6] Pinkse, Jonatan, and Koen Groot. "Sustainable entrepreneurship and corporate political activity: Overcoming market barriers in the clean energy sector." *Entrepreneurship Theory and Practice* 39, no. 3 (2015): 633-654. https://doi.org/10.1111%2Fetap.12055
[7] "Goal 7: Affordable and clean energy." United Nations Development Programme, 2020.
[8] Khosravi, A., Sanna Syri, M. El Haj Assad, and M. Malekan. "Thermodynamic and economic analysis of a hybrid ocean thermal energy conversion/photovoltaic system with hydrogen-based energy storage system." *Energy* 172 (2019): 304-319. https://doi.org/10.1016/j.energy.2019.01.100
[9] Wang, Jianhui, Audun Botterud, Vladimiro Miranda, Cláudio Monteiro, and Gerald Sheble. "Impact of wind power forecasting on unit commitment and dispatch." In *Proc. 8th Int. Workshop Large-Scale Integration of Wind Power into Power Systems*, pp. 1-8. 2009.
[10] Liang, Vernon Yeoh Sheng, Nur Irwany Ahmad, Diyya Hidayah Abd Rahman, Aimi Athirah, Hazwani Zaidi, Saidatul Shema Saad, Nazrul Azril Nazlan, Habibah Mokhtaruddin, and Baseemah Mat Jalaluddin. "Development of Solar Tracking Robot for Improving Solar Photovoltaic (PV) Module Efficiency." *Journal of Advanced Research in Applied Mechanics* 61, no. 1 (2019): 13-24.
[11] Abdullah, Amira Lateef, Suhaimi Misha, Noreffendy Tamaldin, and Mohd Afzanizam Mohd. "Numerical analysis of solar hybrid photovoltaic thermal air collector simulation by ANSYS." *CFD Letters* 11, no. 2 (2019): 1-11.
[12] Khattak, M. A., NS Mohd Ali, NH Zainal Abidin, N. S. Azhar, and M. H. Omar. "Common Type of Turbines in Power Plant: A Review." *Journal of Advanced Research in Applied Sciences and Engineering Technology* 3, no. 1 (2016): 77-100.
[13] Cavazzini, Giovanna, Alberto Santolin, Giorgio Pavesi, and Guido Ardizzon. "Accurate estimation model for small and micro hydropower plants costs in hybrid energy systems modelling." *Energy* 103 (2016): 746-757. https://doi.org/10.1016/j.energy.2016.03.024
[14] Krenn, Jürgen, Helmut Keck, and Manfred Sallaberger. "Small and mid-size pump-turbines with variable speed." *Energy and Power Engineering* 5, no. 2 (2013): 48-54. https://doi.org/10.4236/epe.2013.52A007
[15] Fan, YaJun, AnLe Mu, and Tao Ma. "Modeling and control of a hybrid wind-tidal turbine with hydraulic accumulator." *Energy* 112 (2016): 188-199. https://doi.org/10.1016/j.energy.2016.06.072
[16] Secretariat, REN21. "Renewables 2019 global status report 2019." Paris, France (2019).
[17] Cruz, P., H. M. I. Pousinho, R. Melício, and V. M. F. Mendes. "Optimal coordination on wind-pumped-hydro operation." *Procedia Technology* 17 (2014): 445-451. https://doi.org/10.1016/j.protcy.2014.10.253
[18] Shabani, Masoume, and Javad Mahmoudimehr. "Techno-economic role of PV tracking technology in a hybrid PV-hydroelectric standalone power system." *Applied energy* 212 (2018): 84-108. https://doi.org/10.1016/j.apenergy.2017.12.030
[19] Nyeche, E. N., and E. O. Diemuodeke. "Modelling and optimisation of a hybrid PV-wind turbine-pumped hydro storage energy system for mini-grid application in coastline communities." *Journal of cleaner production* 250 (2020): 119578. https://doi.org/10.1016/j.jclepro.2019.119578
[20] Swanee, P. K., and Akalank K. Jain. "Explicit equations for pipeflow problems." *Journal of the hydraulics division* 102, no. 5 (1976). https://doi.org/10.1061/JYCEAJ.0004542
[21] Mataix, Claudio. *Turbomáquinas hidráulicas: turbinas hidráulicas, bombas, ventiladores*. Editorial ICAI, 1976.
[22] Mataix, Claudio. *Mecánica de fluidos y máquinas hidráulicas*. No. 620.106 M38 2012. Harla, 1982.
[23] Mott, Robert L. *Mecanica de Fluidos 6/e*. Pearson educación, 2006.
[24] Moreau, Vincent, Gontran Bage, Denis Marcotte, and Réjean Samson. "Statistical estimation of missing data in life cycle inventory: an application to hydroelectric power plants." *Journal of Cleaner Production* 37 (2012): 335-341. https://doi.org/10.1016/j.jclepro.2012.07.036
[25] Chapallaz, Jean-Marc, Peter Eichenberger, and Gerhard Fischer. Manual on pumps used as turbines. No. BOOK. Braunschweig, Germany: Vieweg, 1992
[26] Graciano-Uribe, Jonathan, Jorge Sierra, and Edwar Torres-López. "Instabilities and influence of geometric parameters on the efficiency of a pump operated as a turbine for micro hydro power generation: A review." http://dx.doi.org/10.13044/j.sdewes.d8.0321
[27] Munson, Bruce Roy, Theodore Hisao Okiishi, Wade W. Huebsch, and Alric P. Rothmayer. *Fluid mechanics*. Singapore: Wiley, 2013.
[28] Cengel, Yunus. *Heat and mass transfer: fundamentals and applications*. McGraw-Hill Higher Education, 2014.

[29] "Tarifas de energía incluyendo años anteriores" Empresas Públicas de Medellín (EPM), 2020.